Proceedings Solar Activity and its Magnetic Origin
Proceedings IAU Symposium No. 233, 2006
V. Bothmer, B.D. Editor & C.E. Editor, eds.

DOI: 00.0000/X000000000000000X

How does the solar wind blow? Some basic aspects

Nicole Meyer-Vernet

LESIA (CNRS/University Paris 6, Paris 7), Observatoire de Paris, 92190 Meudon, France
email: nicole.meyer@obspm.fr

Abstract. Major properties of the solar atmosphere and wind are not understood. The energy distribution of the solar atmosphere perturbations, over nearly ten orders of magnitude in energy, is close (within one order of magnitude) to a power-law of index -2, even though there is no agreement on the detailed shape. There is no agreed explanation of the origin of the solar wind, either, nor of the fact that the total wind energy flux is independent of speed, latitude, and phase of solar cycle, with an average base flux of 70 W/m^2 - a figure that is similar for a number of other cool stellar winds, and is close to the total observed energy flux of solar atmosphere perturbations. A major theoretical difficulty is that both coronal heating and wind production depend fundamentally on the heat flux, and the solar atmosphere is not collisional enough for classical transport theory to hold. Heat transport thus behaves non classically and the particle velocity distributions may have significant high energy tails, which should dramatically affect coronal heating and solar wind acceleration, in a way that is outside the scope of standard MHD.

Keywords. solar wind, Sun: particle emission, Sun: atmosphere, Sun: corona, Sun: flares, stars: mass loss, MHD

1. Introduction

The solar atmosphere and wind are still not understood despite the increasing flow of high-quality data, sophisticated theories and empirical models. The number of theories of coronal heating increases at the same rate as the data, and, rather ironically, the fast wind - which fills most of the heliosphere near solar activity minimum, is the most difficult to explain, although it is the most stationary and its geometry is simpler.

Early solar wind theories were based on a thermally driven wind. Unfortunately, neither the original Parker (1958) theory assuming a constant temperature (i.e. an infinite heat flux), nor the subsequent fluid models based on the classical (collisional) heat flux can reproduce the observed high speed wind. This failure led to a new paradigm: Alfven (or cyclotron) waves heating the corona and driving the wind (see Cranmer 2002). Despite much effort, the required waves have not been observed, and there is still no successful theory of their dissipation. Despite these inadequacies, the wave paradigm has led to forget a suggestion by Olbert (1981) that the wind may be suprathermally driven, due to the large non-classical heat flux produced by suprathermal electrons suggested to be present in the low corona.

Before discussing new developments that may support a suprathermally driven wind, consider first the solar atmosphere.

2. Solar atmosphere perturbations

Heating the corona requires but a fraction $10^{-6} - 10^{-5}$th of the solar luminosity; however, since this heating requires energy to flow from cold to hot regions, it cannot involve the classical heat flux. The heating process has not been identified, even though a large number of theories have been proposed and we know that the magnetic field plays a key role (see Klimchuk 2006).

This problem may be related to the perturbations observed in the solar atmosphere - attributed to the magnetic field, too, even outside the so-called active regions. These transient events have been given various names according to their size, appearance and wavelength of observation, and are observed at widely different energies, from $10^{15.7}$ to 10^{25} J or more, over the whole solar surface. While the low energy events are detected from Doppler-shifts in ultraviolet lines - attributed to bulk flows of matter - the high energy events are detected as X-rays brightenings - attributed to Bremsstrahlung radiation from energetic electrons. The difficulties of remote sensing observation, however, often make similar phenomena appear different, and vice-versa.

Figure 1 (from Meyer-Vernet 2006) is a compilation of the average number of transient events dN, observed per second per unit area on the Sun in the energy range dW, versus the energy W (from Crosby *et al.* 1993; Shimizu 1995; Krucker & Benz 1998; Aschwanden *et al.* 2000; Aschwanden & Parnell 2002; Winebarger 2002). The distributions over restricted energy ranges are of the form $dN/dW \propto 1/W^{\alpha}$, with $1.5 < \alpha < 3$, with a trend for α to increase as energy decreases. However all authors do not agree on what they mean by 'event' (see Buchlin *et al.* 2006) and there are many observational bias in the determination of the event rate and energy, so that the power law index appears to depend on the observational scheme.

The power-law index has attracted some attention since small-scale magnetic activity has been proposed to be responsible of coronal heating (see Parker 1991), and the total energy of the observed events - that we call 'flares' for short

$$W_{flares} = 4\pi R_{\odot}^2 \times \int_{W_{\min}}^{W_{\max}} dW \ \ W \ \ dN/dW \tag{2.1}$$

($\propto 1/W_{\min}^{\alpha-2}$ if $\alpha > 2$ and $W_{\min} \ll W_{\max}$) may be sufficient for coronal heating outside active regions if $W_{\min}$ is small enough and α large enough - a question that is not settled.

Anyway, it is remarkable that a single power-law distribution (Figure 1)

$$dN/dW \simeq 3/W^2 \ \ \mathrm{s^{-1}\ m^{-2}\ J^{-1}} \qquad \text{for} \qquad 10^{15.7} < W < 10^{25}\ \mathrm{J} \tag{2.2}$$

approximates (to better than a factor of ten) the superposition of all these data, over nearly ten orders of magnitude in energy. The distribution (2.2) has the fundamental property that the energy contained in each energy decade is independent of energy (being equal to $3 \ln 10 \simeq 7$ W/m^2). Integrating (2.1) with the distribution (2.2) from $W_{\min} = 10^{15}$ J to $W_{\max} = 10^{25}$ J yields the total energy flux:

$$W_{flares}/(4\pi R_{\odot}^2) \simeq 3. \times \ln(W_{\max}/W_{\min}) \simeq 70 \ \mathrm{W\ m^{-2}} \tag{2.3}$$

weakly dependent of the extremities of the distribution. We shall return to this figure later.

Power law distributions are observed in a number of contexts, and their ubiquity has aroused much interest in widely different fields. Prominent examples are cosmic rays and Earthquakes, which have power-law energy distributions of index -2.5 and -2 respectively, over nearly ten orders of magnitude in energy. The same is true of a number of other phenomena, from the diameter of moon craters, to web hits, ... the occurence of words in the novel *Moby Dick* and the number of species in genera of flowering plants, all having power law indices in the range $1.5 - 3$ (see Newman 2005).

Several tentative explanations have been proposed. The two most successful ones are based respectively on the *Yule* process and on critical phenomena. The Yule process

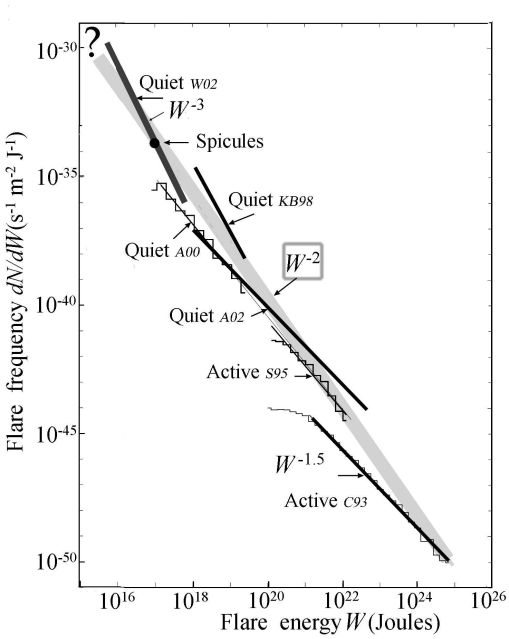

Figure 1. Frequency distribution of transient events in the upper solar atmosphere as a function of energy, in quiet and active regions (from studies cited in the text and labelled by first letter of author's name and date). The superposition of power law distributions determined in different energy ranges (dark grey lines) is close to a power law of index -2 (thick grey line).

concerns quantities that increase in proportion to their number ('rich gets richer'). It is widely used in biology, but may be applied in a modified form to magnetic structures and plasma particles; a simple version is the Fermi acceleration; note that first-order Fermi acceleration in shocks produces a particle energy spectrum $\propto W^{-2}$ (see Longair 1997). On the other hand, critical phenomena, related to phase transitions (forced and/or self-organised criticality, see Bak 1987) have raised much excitement in the last decades.

Whatever the explanation of the spectrum of solar perturbations (if there is a generic one), there is no agreement on the microscopic physics, except for the fact that it is mediated by the magnetic field.

3. Solar wind total energy flux and other cool stellar winds

The Ulysses spacecraft has produced solar wind *in situ* measurements in three dimensions since nearly 15 years. The orbital period is about half a solar cycle and the pole-to-pole transit near perihelion (near 1.3 AU) takes less than a year (alternatively at solar activity minimum and maximum), so that each such passage yields the solar wind variation with heliocentric latitude - other parameters being roughly constant. These results (see Issautier *et al.* 2000) show that the slow and fast wind, despite their wide differences in source, geometry, speed, density, temperature and composition, have a momentum flux differing by only 20%, and have virtually the same energy flux, independent of latitude, at both solar activity minimum and maximum:

$$\rho V \times \left(\frac{V^2}{2} + \frac{M_\odot G}{R_\odot}\right) \simeq 70 \times \left(\frac{R_\odot}{r}\right)^2 \ \mathrm{W/m^2} \tag{3.1}$$

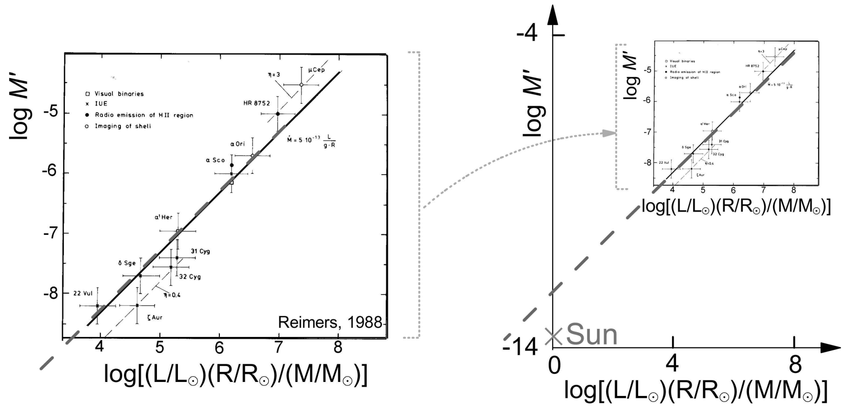

Figure 2. An empirical relation between the mass loss rate of stars (in units of $M_\odot$/year) and the ratio of their luminosity to their gravitational potential (normalised to solar values).

where ρ and V are the mass density and speed at a large distance r (where the enthalpy and heat flux are negligible), $M_\odot$ and $R_\odot$ are respectively the solar mass and radius, and G is the gravitational constant. Similar results were derived from Helios measurements at low latitudes (Marsch 1991; Schwenn 1991). The average energy flux at the base of the wind is therefore:

$$\frac{W_{\odot wind}}{4\pi R_\odot^2} \simeq \frac{M'_\odot}{4\pi R_\odot^2} \times \left(\frac{V^2}{2} + \frac{M_\odot G}{R_\odot}\right) \simeq 70 \text{ W/m}^2 \tag{3.2}$$

$M'_\odot$ being the solar mass loss rate and V the terminal speed. This turns out to be close to the total energy flux (2.3) of solar 'flares' derived from Figure 1. Comparing to the solar luminosity $L_\odot$, one sees that the total energy loss in the wind is $W_{\odot wind} \simeq 10^{-6} L_\odot$.

It is interesting to compare these values with two empirical results derived for cool giant stars. Figure 2 (left) shows a widely quoted relation (Reimers 1988) between the mass loss M' in the winds and the ratio of the stars' luminosity to the base gravitational energy MG/R (normalised to solar values), for stars of mass M and radius R. This empirical relation is also met by other kinds of cool stars and by the Sun with an accuracy of one order of magnitude, so that the relation holds over ten orders of magnitude in mass loss rate (Figure 2, right). Such a relation is suggested by dimensional arguments and is not unexpected since the wind is ultimately powered by the star's luminosity and restrained by the gravitational attraction; its fundamental significance, however, is not a trivial matter since these winds are not radiatively driven.

A hint may be obtained by noting that since the terminal kinetic energy $V^2/2$ of these winds is of the same order of magnitude of (or smaller than) the gravitational energy at the base MG/R, the empirical law shown in Figure 2 may be rearranged as $W_{wind} \sim 2 \times 10^{-5} \times L$. This suggests that the engines powering these stellar winds - including the Sun's - have a similar efficiency, of order of magnitude $10^{-6} - 10^{-5}$, in terms of the stellar luminosity.

For the same sample of stars, the radiative fluxes differ much less than the wind mass fluxes, and the total wind energy fluxes at the base $W_{wind}/4\pi R^2$ are found to be similar within one order of magnitude, i.e. (Reimers 1988)

$$\frac{W_{wind}}{4\pi R^2} \simeq \frac{M'}{4\pi R^2} \times \left(\frac{V^2}{2} + \frac{MG}{R}\right) \sim 10^2 \text{ W/m}^2 \tag{3.3}$$

This is close to the solar value (3.2), and means that the expression (3.3) holds over 10

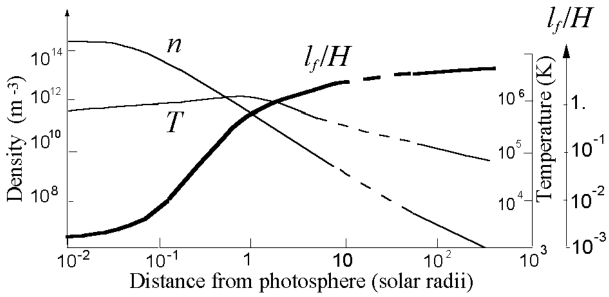

Figure 3. Electron density, temperature and mean free path (normalised to the density scale height) versus distance in the fast wind.

orders of magnitude in mass loss rate. So, not only is the energy flux in the wind similar for the slow and fast solar wind, but it is the same for a number of other stars of much larger mass loss rate.

4. Non-classical heat flux

The energy per unit mass of a wind of speed V and temperature T at distance r is $V^2/2 + 5k_BT/m_p - MG/r$ (m_p is the proton mass). In the absence of *ad-hoc* heating or wave flux and of radiation loss, the wind energy balance thus reads

$$V^2/2 + 5k_BT/m_p - MG/r + Q/(\rho V) = \text{ constant} \tag{4.1}$$

with distance, where ρV and Q are respectively the mass flux and heat flux at distance r. Let us apply this equality between the base of the wind and a large distance r. Since both the enthalpy and the large distance heat flux term are negligible compared to the terminal kinetic energy, the ratio of the heat flux to the mass flux at the base of the wind is $Q_0/(\rho_0 V_0) \simeq V^2/2 + MG/R$ (for a star of mass M and radius R and a wind of terminal speed V). Applying this equation to the whole star's surface (with $\rho_0 V_0 = M'/4\pi R^2$), shows that the average energy loss in the wind per unit stellar surface $W_{wind}/4\pi R^2$ equals the average heat flux at the base. Equations (3.2)-(3.3) thus suggest that the average heat flux at the base of the wind may be similar for the Sun and many other stars over 10 orders of magnitude in mass loss.

Calculating the heat flux thus appears crucial for understanding these winds. In the case of the Sun, the classical collisional heat flux (Spitzer-Harm) is too small for powering the fast wind (and anyway, it points in the wrong direction) - which led to the paradigm of a wave powered wind. The classical heat flux, however, only holds in a collisional medium. Figure 3 shows the electron mean free path (normalised to the scale height), as a function of distance from the solar surface in the fast wind. One sees that in the corona and the wind, the ratio of the free path to the scale height is larger than 10^{-3}.

It is well known that in this case, classical transport theory is invalid (see for example Shoub 1988), so that the heat flux must be calculated differently. Indeed, it is only in a neutral gas that classical transport theory holds when the mean free path is smaller than the temperature scale height. The condition is much more stringent in a plasma because charged particles interact via the (long range) Coulomb force. Indeed, the close encounter distance r_L for two charges e is given by equating the potential energy $e^2/(4\pi\epsilon_0 r_L)$ to the kinetic energy $mv^2/2$, so that the collision cross section varies approximately as $r_L^2 \propto v^{-4}$, whence the free path $\propto v^4$. Hence, when the *mean* free path equals the scale height, a particle moving, say, three times faster than average has a free path greater by

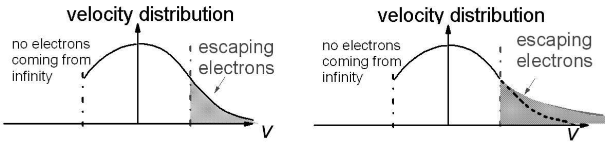

Figure 4. Sketch of the origin of the heat flux in a collisionless plasma (left) and of its increase as the electron velocity distribution develops a suprathermal tail.

two orders of magnitude. This precludes uniform convergence of the expansions used to derive the usual transport equations. As a result, in the solar transition region, corona, and wind, the heat flux is not classical (see for example Shoub 1983).

In other words, even when the thermal particles are collisional, the suprathermal ones are not, and since heat is mainly carried by suprathermal electrons, the heat flux is non local, and must be calculated with a kinetic picture.

Figure 4 (left) sketches the origin of the heat flux in a collisionless wind. The fast electrons are escaping from the interplanetary electric potential arising from the difference in mass between electrons and ions; since in the absence of collisions, there are no electrons of such fast speed coming towards the Sun, the velocity distribution exhibits an asymmetry which produces an outward heat flux directly related to the bulk speed. A well-known *ansatz* for the non-collisional heat flux with a maxwellian is (Hollweg 1974)

$$Q_{NC} \simeq \alpha \times nVk_BT \tag{4.2}$$

where n, V and T are respectively the mean electron number density, velocity and temperature, and α is a numerical factor $\sim 1.5 - 15$.

Note that this expression is formally similar to the heat flux of a polytrope wind - a basically different approximation. Polytrope modelizations ($P \propto \rho^\gamma$) are often used for media whose heat flux is not given by the classic (Spitzer-Harm) value; this is formally equivalent to assuming a heat flux given by (4.2) with $\alpha = \gamma/(\gamma-1) - 5/2$. Extreme cases are $\gamma = 5/3$ ($\Rightarrow Q = 0$: adiabatic) and $\gamma = 1$ ($\Rightarrow Q \to \infty$: isothermal).

However in a weakly collisional plasma, neither the classical collisional heat flux nor the non-collisional one holds *a priori*, and a kinetic calculation is required.

5. Non-maxwellian velocity distributions and consequences

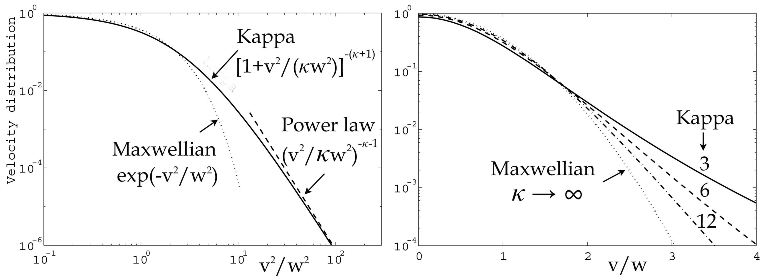

Figure 5. Left: Kappa distribution compared to a Maxwellian and to a power law. Right: Kappa distributions with different values of κ; the suprathermal tail increases as κ decreases. (Adapted from Meyer-Vernet 2001.)

Since the fast particles are nearly collisionless, they are easily accelerated and tend to produce suprathermal tails in the velocity distributions; in the solar atmosphere, the large gradients conspire to produce such tails. Since many acceleration processes produce

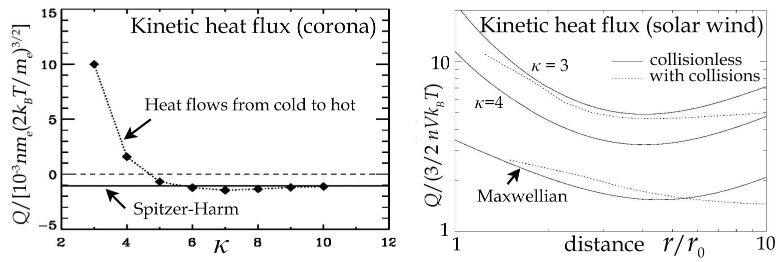

Figure 6. Kinetic calculations of the heat flux in the solar corona (left) and in the wind acceleration region (right) with Kappa velocity distributions. Left: Normalized heat flux versus κ in a thin slab of corona (Landi & Pantellini 2001); for $\kappa < 5$, heat flows towards increasing temperature. Right: Normalized heat flux versus normalized heliocentric distance in the wind acceleration region (Zouganelis *et al.* 2005a); the (outward) heat flux increases strongly as κ decreases.

power laws, one expects the distributions to be maxwellian at low speeds (for which the particles are collisional) and power-law at larger speeds (for which the particles are collisionless). A convenient model for such distributions is the Kappa function (Figure 5), which reduces to a Maxwellian as $\kappa \to \infty$. Such distributions are ubiquitous in space plasmas; they have been observed *in situ* for both ions and electrons in the solar wind and in the environments of the Earth, Jupiter, Saturn, Uranus, and Neptune.

The presence of a suprathermal tail in the coronal proton velocity distribution is still controversial (Kohl 2005). A suprathermal tail for electrons in the upper solar atmosphere has been proposed long ago by Olbert (1981), as such a tail is ubiquitous in the solar wind (see for example Maksimovic *et al.* 2005). This would resolve many observational inconsistencies (see for example Scudder 1992b; Esser & Edgar 2000; Chiuderi & Chiuderi Drago 2004). A number of theories have been suggested to produce such distributions (see Collier 2004; Vinas *et al.* 2000; Vocks & Mann 2003). Given the numerous acceleration processes at work in the solar atmosphere and the paucity of collisions, the production of suprathermal tails would not be surprising. This may occur during the events shown in Figure 1, by conversion of magnetic energy into particle energy.

If the velocity distributions in the upper solar atmosphere do have suprathermal tails, a number of major consequences follow. First of all, many observations should be reinterpreted since virtually all solar observations implicitely assume that the velocity distributions are Maxwellian (or bi-maxwellian) in their proper frame.

Second, the heat flux behaves non-classically. Scudder (1992a) has shown that without collisions, suprathermal particles - because of their greater scale height - survive in greater proportion than the thermal ones at higher altitudes in the solar gravitational field, producing a *velocity filtration* which makes the kinetic temperature increase upwards, and proposed that this might explain coronal heating. This calculation, however, neglects collisions, which is not acceptable in the transition region. Figure 6 (left, from Landi & Pantellini 2001) shows the heat flux versus κ in a slab of the solar corona, taking collisions into account, from a kinetic simulation which does not suffer of the deficiencies affecting Fokker-Planck approximations since it is based on a numerical integration of the particle motion. Whereas for $\kappa > 5$ the heat flux is close to the classical (Spitzer-Harm) collisional value, for smaller κ, the heat flux changes of sign and strongly increases. The simulation shows, however, that $\kappa < 4$ is needed for the corona to be heated in this way.

Figure 6 (right, from Zouganelis *et al.* 2005a) shows the heat flux calculated in the solar wind acceleration region for different values of κ with both a kinetic collisionless calculation (Zouganelis *et al.* 2004, continuous lines) and a numerical simulation taking collisions into account (Landi & Pantellini 2003, dotted lines). The similarity between both results is not surprising since the heat flux is produced by suprathermal electrons which are collisionless. With a maxwellian electron velocity distribution, the heat flux is close to the collisionless approximation (4.2) (with $\alpha \simeq 4$), and is too small to produce the fast wind. As κ decreases, however, the heat flux increases strongly due to the larger suprathermal tail, and becomes sufficient to power the fast wind if κ is small enough, producing a suprathermally driven wind (Zouganelis *et al.* 2005b).

References

Aschwanden, M. J. et al. 2000, *ApJ.* 535, 1047

Aschwanden, M. J. & Parnell, C. E. 2002, *ApJ.* 572, 1048

Bak, P., Tang, C. & Wiesenfeld, K. 1987, *Phys. Rev. Lett.* 59, 381

Buchlin, E., Galtier, S., Velli, M. 2006, *Astron. Astrophys.* 436, 355

Chiuderi, C. & Chiuderi Drago, F. 2004, *Astron. Astrophys.* 422, 331

Collier, M. R. 2004, *Adv. Space Res.* 33, 2108

Cranmer, S.R. 2002, *Space Sci. Rev.* 101, 229

Crosby, N.B., Aschwanden, M.J. & Dennis, B.R. 1993, *Solar Phys.* 143, 275

Esser, R. & Edgar, R.J. 2000, *ApJ.* (Letters) 532, L71

Hollweg, J. V. 1974, *J. Geophys. Res.* 79, 3845

Kohl, J.L. et al. 2005, *AGU Fall meet.*

Klimchuk, J.A. 2006, *Solar Phys.* 234, 41

Krucker, S. & Benz, A.O. 1998, *ApJ.* (Letters) 501, L213

Landi, S. & Pantellini, F.G. 2001, *Astron. Astrophys.* 372, 686

Landi, S. & Pantellini, F.G. 2003, *Astron. Astrophys.* 400, 769

Longair, M.S. 1997, *High energy Astrophysics* (Cambridge University Press)

Maksimovic, M. et al. 2005, *J. Geophys. Res.* 110, 9104

Marsch, E. 1991, in: R. Schwenn and E. Marsch (eds.), *Physics of the Inner Heliosphere* (Springer), vol. 2, p. 45

Meyer-Vernet, N. 2001, *Planet. Space Sci.* 49, 247

Meyer-Vernet, N. 2006, *Basics of the Solar Wind* (Cambridge University Press)

Newman, M.E.J. 2005 *Contemp. Phys.* 46, 323

Olbert, S. 1981, in: T.D. Guyenne & G. Levy (eds.), *Plasma Astrophysics* (ESA SP-161), p. 359

Parker, E.N. 1958, *ApJ.* 128, 664

Parker, E.N. 1991, *ApJ.* 372, 719

Reimers, D. 1988, in: L. Bianchi and R. Gilmozzi (eds.), *Mass Outflows from Stars and Galactic Nuclei* (Kluwer), p. 25

Schwenn, R. 1991, in: R. Schwenn and E. Marsch (eds.), *Physics of the Inner Heliosphere* (Springer), vol. 1, p. 99

Scudder, J.D. 1992, *ApJ.* 398, 299

Scudder, J.D. 1992, *ApJ.* 398, 319

Shimizu, T. 1995, *PASJ* 47, 251

Shoub, E.C. 1983, *ApJ.* 266, 339

Shoub, E.C. 1988, in: V. J. Pizzo et al. (eds.), *Proceed. Solar Wind 6*, NCAR TN- 306 (Boulder), p. 59

Vinas, A. F. et al. 2000, *ApJ.* 528, 509

Vocks, C. & Mann, G. 2003, *ApJ.* 593, 1134

Winebarger, A.R. 2002, *ApJ.* 565, 1298

Zouganelis, I. et al. 2004, *ApJ.* 606, 542

Zouganelis, I. et al. 2005a, in: B. Fleck and T.H. Zurbuchen (eds.), *Proceed. Solar Wind 11 - SOHO 16*, ESA SP-592 (Noordwijk), p. 171

Zouganelis, I. et al. 2005b, *ApJ.* (Letters) 626, L117